Theoretical aspects of higher-order truncations in solid-state nuclear magnetic resonance

M. Goldman
Direction des Sciences de la Matière DRECAM/SPEC, Commissariat à l'Energie Atomique, Saclay, 91191 Gif-sur-Yvette Cedex, France

P. J. Grandinetti, A. Llor,[a] Z. Olejniczak,[b] and J. R. Sachleben
Materials Sciences Division, Lawrence Berkeley Laboratory, 1 Cyclotron Road, Berkeley, California 94720 and Department of Chemistry, University of California, Berkeley, California 94720

J. W. Zwanziger
Department of Chemistry, Indiana University, Bloomington, Indiana 47405

(Received 10 April 1992; accepted 9 September 1992)

Recent experimental developments of high-resolution NMR in solids (for example, double rotation and dynamic-angle spinning) address the reduction of second-order line broadening effects, particularly in systems involving quadrupolar nuclei such as ^{23}Na, ^{17}O, ^{27}Al, and ^{14}N. However, some aspects of the theoretical description of these systems have not been clearly understood; in particular, the various procedures available to truncate the interactions give incompatible results. We present a general framework, based on static perturbative methods, which provides a natural procedure to derive the correct Hamiltonian for higher-order effects in irreducible tensor form. Applications of this method to coherent averaging techniques (sample motion or radio-frequency irradiation) are described and compared to previous treatments based on average Hamiltonian theory.

I. INTRODUCTION

The importance of NMR stands in its ability to provide physicochemical information on a sample through the measurement of internal nuclear spin interactions. However, these interactions are not observed alone but in conjunction with the Zeeman interaction, which truncates them. Truncation procedures are well known from the early days of quantum mechanics and have found straightforward and widespread applications in NMR.[1,2]

One of the consequences of truncation is the anisotropy effects in the NMR of solids, namely, the dependence of the spectrum on the orientation of the crystal in the magnetic field.[1–3] A considerable amount of work has been devoted to devising experimental techniques that suppress these anisotropy effects, which typically cause broadening of the resonances in polycrystalline and amorphous samples to the extent that resolution (and thus information content) is lost.[2,3] These developments were first initiated by Andrew and Lowe in 1958 with the magic-angle spinning (MAS) technique.[4,5] Important landmarks in the stream of improvements, due to Waugh and co-workers, were the WAHUHA sequence, and the introduction of average Hamiltonian theory (AHT) as the main tool to describe the effect of time-dependent interactions.[6,7] More refinements have been added recently with the double rotation (DOR) (Ref. 8) and dynamic-angle spinning (DAS) (Refs. 9 and 10) methods. As these techniques spread to many research groups, the connected concepts of irreducible tensors and AHT (Refs. 11 and 12) have modified the way NMR spectroscopists envision some theoretical aspects in their field. Irreducible tensors can be very useful in simplifying calculations, and also for providing a more intuitive understanding of the coherent averaging processes (which are based on combinations of rotations). At the same time, and because of its natural formulation in terms of irreducible tensor expressions, AHT has been gradually applied to almost every kind of situation, sometimes abusively.

Many authors have pointed out that AHT, at variance with other theories, cannot properly describe some experimental results. In general, such situations seem most likely to be found when the effects of second- and higher-order truncated interactions are not negligible. The long-time behavior of a spin system under continuous or pulsed irradiation is a well-known example that has stirred some controversy in the last decade as to the correct theoretical tool to describe it. The time evolution is eventually controlled by higher-order effects due to nonsecular terms. The various fundamental questions that arise when dealing with this problem have been reviewed recently.[13]

Another case of discrepancies arises in the coherent averaging of the anisotropies due to second-order effects, for instance, when a quadrupolar coupling is not negligible compared to the Zeeman interaction.[14] Although such situations have been explored for many decades, they have been a source of confusion. Fortuitously, these misconceptions have yielded only slight discrepancies between theory and experiment. However, the recent development of specific methods such as DAS and DOR, which are engineered to reduce second-order effects, mandates a clarification of the associated theoretical aspects.

[a] On leave from Direction des Sciences de la Matière DRECAM/SCM, Commissariat à l'Energie Atomique, Saclay, 91191 Gif-sur-Yvette Cedex, France.

[b] On leave from Institute of Nuclear Physics, Radiospectroscopy Division, Radzikowskiego 152, 31-342 Krakow, Poland.

Most of the difficulties found in the literature can be traced back to the procedure used to truncate the quadrupolar interaction by the Zeeman field when the sample is static: Many authors convert the interaction to the rotating frame, where it becomes time-dependent, and then apply AHT to obtain the truncated Hamiltonian in the rotating frame.[14–17] In second order, the resulting interaction contains off-diagonal elements with respect to the Zeeman interaction that happen to vanish through a second truncation by the first-order perturbation Hamiltonian.[14] However, if the sample rotates fast enough at the magic angle to average out the first-order term, two contradictory predictions for the second-order broadening arise, depending on whether the nonsecular terms in the second-order expansion are retained or discarded. At variance with this description, an analysis based on static perturbation theory (SPT) does not predict such effects.[18] Other minor disagreements between the SPT and AHT approaches may also be expected and indeed have been reported, but no arguments were given to explain them.[14]

To highlight the effect of these nonsecular terms in AHT, we have performed a set of simulations for the NMR transition of a single-crystal sample, containing equivalent uncoupled quadrupolar nuclei of spin $\frac{3}{2}$, and spinning around the magic angle at various speeds. The computational details are given in the Appendix. The spectra in Fig. 1 were calculated using three different methods: a full diagonalization procedure (referred to as "exact") and two perturbation methods carried to second order (SPT and AHT). The results clearly show the failure of AHT to provide even an approximate description of the system when the spinning speed becomes comparable to the quadrupolar coupling, while SPT is in good agreement throughout the range of experimental parameters.

The aim of this work is to give a general and coherent framework for treating second- and higher-order truncation effects that commonly arise in NMR. Although this may be done by dynamic methods (i.e., by going to the rotating frame), it is much simpler to use static diagonalization methods, since the Hamiltonian is time independent. The usual perturbation expansions for the diagonalization are formulated in terms of matrix elements.[19] We shall, however, reformulate these in terms of operators decomposed into irreducible tensors. Two different methods, SPT and Van Vleck transformation (VVT), will be given; SPT is useful for systems with a finite number of levels and VVT is adapted to highly degenerate (e.g., dipolar broadened) systems. Then we shall generate effective Hamiltonians and interaction frames that are suitable to analyze averaging experiments. The effective Hamiltonian yielded by these static methods can be used to analyze some aspects of common coherent averaging experiments, either by radio-frequency irradiation or sample rotation. Finally, we will discuss the proper conditions under which AHT describes higher-order truncations and the difficulties involved in extending this approach to include sample motion.

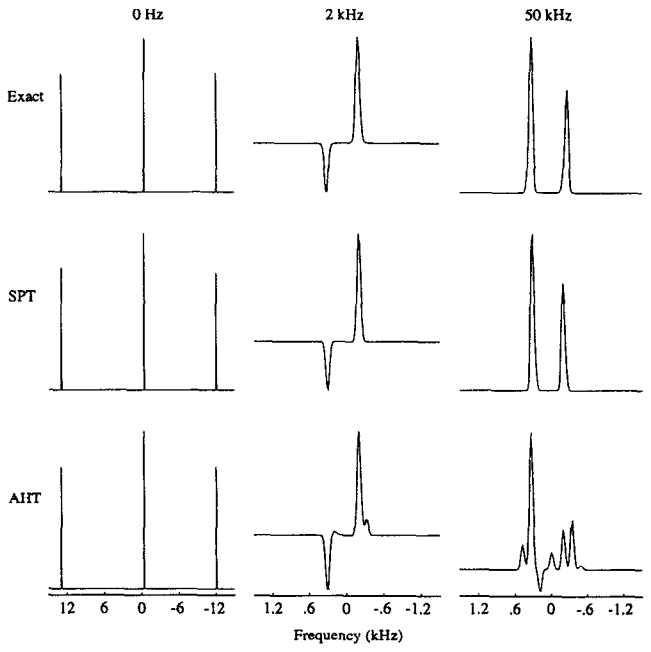

FIG. 1. Exact, SPT, and AHT simulations of the NMR transitions of a single-crystal sample, containing equivalent uncoupled quadrupolar nuclei of spin $\frac{3}{2}$, and spinning around the magic angle at three different speeds. The spinning speeds ($\nu_R=0$, 2, and 50 kHz), are selected to fall in the ranges $0-\nu_Q^2/\nu_Z$, $\nu_Q^2/\nu_Z-\nu_Q$, and $\nu_Q-\nu_Z$, showing three different behaviors of the AHT. The SPT simulations were performed in the laboratory frame using a nontilted diagonal Hamiltonian [$V=1$ in Eqs. (6) and (7)] containing the Zeeman interaction and the quadrupolar interaction truncated to second order [Eqs. (10), (12), and (13)]. The AHT simulations were performed in the rotating frame using only the first- and second-order truncated quadrupolar interaction including off-diagonal elements as given in Eq. (65). The dwell times are chosen to avoid folding of spinning sidebands in the AHT and SPT approximations, but it is taken 5 times smaller than the Zeeman period for all the exact simulations to avoid aliasing of the various multiple quantum transitions. In the later case we preferred to reduce the dwell time (increasing the computation time considerably) instead of implementing some kind of filtering which would then make the code different from that of the other cases. The continuous motion of the sample is approximated as a succession of discrete evenly distributed orientations of duration Δt. A Δt of $t_Z/10$ was employed in the exact $\nu_R=2$ and 50 kHz simulations. A Δt of $t_R/20$ was employed in the SPT and AHT $\nu_R=2$ and 50 kHz simulations. Only the region of the central $\pm\frac{1}{2}$ transition is shown for the $\nu_R\neq 0$ spectra. Additional details of the calculation are given in the Appendix.

II. STATIC PERTURBATION THEORY IN TERMS OF IRREDUCIBLE TENSOR OPERATORS

In its usual formulation, SPT (Ref. 19) provides an expansion for the eigenvalues and eigenstates of a perturbed operator (which in our case will be the internal Hamiltonian). The results to second order are summarized by the following well-known formulas (limited here to nondegenerate systems):

$$H=H^{(0)}+H^{(1)}, \tag{1}$$

$$H|v_j\rangle=E_j|v_j\rangle, \quad H^{(0)}|j\rangle=E_j^{(0)}|j\rangle, \tag{2}$$

$$E_j=E_j^{(0)}+E_j^{(1)}+E_j^{(2)}+\cdots, \quad |v_j\rangle=|j\rangle+|v_j^{(1)}\rangle+\cdots, \tag{3}$$

$$E_j^{(1)}=\langle j|H^{(1)}|j\rangle, \tag{4}$$

$$E_j^{(2)}=\sum_{k\neq j}\frac{\langle j|H^{(1)}|k\rangle\langle k|H^{(1)}|j\rangle}{E_j^{(0)}-E_k^{(0)}},$$

$$|v_j^{(1)}\rangle=\sum_{k\neq j}\frac{\langle k|H^{(1)}|j\rangle}{E_j^{(0)}-E_k^{(0)}}|k\rangle. \tag{5}$$

This procedure can be summarized in operator form by the equations:

$$H=VDV^{\dagger}, \tag{6}$$

$$D=H^{(0)}+D^{(1)}+D^{(2)}+\cdots, \quad V=1+V^{(1)}+\cdots, \tag{7}$$

$$D^{(1)}=\sum_j |j\rangle E_j^{(1)}\langle j|, \tag{8}$$

$$D^{(2)}=\sum_j |j\rangle E_j^{(2)}\langle j|, \quad V^{(1)}=\sum_j |v_j^{(1)}\rangle\langle j|, \tag{9}$$

where D and $D^{(n)}$ are diagonal operators and V is a unitary transformation. These equations give the operators in terms of matrix elements and, in general, there is no convenient way of simplifying them. An expansion of the outer products in terms of irreducible tensors[20,21] could be developed but the calculation would be awkward and the result would not give any intuitive understanding of the system. However, in the case of NMR, the Zeeman interaction $H^{(0)}$ is a linear combination of I_z angular momentum operators, and $H^{(1)}$ is the superposition of the various local interactions which have simple expressions in irreducible tensor form. The matrix element $\langle k|H^{(1)}|j\rangle$ in Eqs. (1)–(5) can thus be simplified using the selection rules associated with irreducible tensors, and eventually pure irreducible tensor expansions for the D and V matrices can be found. We shall demonstrate this procedure on two common cases of second-order effects.

In our first example, we deal with probably the simplest case found in NMR: a single nucleus of spin greater than $\frac{1}{2}$, with a quadrupolar coupling smaller than the Zeeman interaction. We have

$$H^{(0)}=H_Z=-\omega_Z I_Z, \tag{10}$$

$$H^{(1)}=H_Q=\omega_Q\sum_m (-1)^m R_{2-m}T_{2m}, \tag{11}$$

where, following the notation of Haeberlen,[12] the quadrupolar interaction is expanded using Z as quantization axis. The R_{2m} are the lattice parts and depend on the orientation in the lab frame of the principal axis of the interaction. Inserting these expressions into Eqs. (1)–(9), we find

$$D^{(1)}=\omega_Q R_{20}T_{20}, \tag{12}$$

$$D^{(2)}=\frac{\omega_Q^2}{\omega_Z}\sum_{m>0}\frac{R_{2m}R_{2-m}[T_{2-m},T_{2m}]}{m}, \tag{13}$$

$$V^{(1)}=\frac{\omega_Q}{\omega_Z}\sum_{m\neq 0}(-1)^m\frac{R_{2-m}T_{2m}}{m}. \tag{14}$$

The first-order expression, Eq. (12), is the well-known truncated Hamiltonian and its derivation from Eq. (8) is straightforward. The calculation of $D^{(2)}$ and $V^{(1)}$ is given in the Appendix. The result is much more concise than the usual derivations,[1,2,3,18] in which the shifts to second order are given separately for each energy level and it is similar to that given by AHT (Refs. 14–17) except for the restriction of $D^{(2)}$ to diagonal elements. Using the Clebsch–Gordan series[20,21] in Eq. (13), the lattice products of second-rank tensors may of course be rewritten as combinations of tensors of ranks 0, 2, and 4, while the spin commutators will yield only ranks 1 and 3.[17] In cases of half-integer spins for which the quadrupolar interaction is large compared to the achievable bandwidths of radio frequency (rf) pulses, it may also be useful to restrict the spin part to the central $\pm\frac{1}{2}$ transition by introducing the corresponding pseudo-spin $\frac{1}{2}$ operator.[17]

Another example is the influence, in second order, of the quadrupolar interaction of a spin $S>\frac{1}{2}$ on the heteronuclear dipolar coupling between S and a nucleus $I=\frac{1}{2}$, for example, ^{13}C and ^{14}N.[22] We assume the dipolar interaction to be much smaller than the quadrupolar interaction. This case has been rather extensively explored using SPT (Refs. 22–31) and AHT (Ref. 32) but the results were not given in terms of irreducible tensors. The $H^{(0)}$ and $H^{(1)}$ terms of the Hamiltonian read as

$$H^{(0)}=H_Z^I+H_Z^S=-\omega_I I_Z-\omega_S S_Z, \tag{15}$$

$$H^{(1)}=H_Q^S+H_D^{IS}, \tag{16}$$

$$H_Q^S=\omega_Q\sum_m (-1)^m R_{2-m}^Q T_{2m}^S, \tag{17}$$

$$\begin{aligned}H_D^{IS}&=\omega_D\sum_m (-1)^m R_{2-m}^D T_{2m}^{IS}\\&=\omega_D\sum_m (-1)^m R_{2-m}^D\Big(\sum_n \langle 1\,1\,n\,m-n|1\,1\,2\,m\rangle\\&\quad\times T_{1n}^I T_{1m-n}^S\Big),\end{aligned} \tag{18}$$

where H_Z^I and H_Z^S are the Zeeman interactions for spins I and S, respectively, H_Q^S is the spin S quadrupolar interaction, H_D^{IS} is the I-S dipolar interaction, and $\langle 1\,1\,n\,m-n|1\,1\,2\,m\rangle$ is the Clebsch–Gordan coefficient $\langle j_1 j_2 m_1 m_2|j_1 j_2 J M\rangle$. To first order the truncated interactions are given by the usual $m=0$ and $n=0$ terms [H_Q^S gives the same expressions as Eqs. (12)–(14)], but to second order we find an uncoupled quadrupolar contribution, a negligible second-order dipolar contribution, and a significant cross term between H_Q^S and H_D^{IS}, which reads as

$$D_{QD}^{(2)}=\sqrt{3/2}\,\frac{\omega_D\omega_Q}{\omega_S}(R_{2-1}^D R_{21}^Q+R_{21}^D R_{2-1}^Q)T_{10}^I T_{20}^S. \tag{19}$$

Again, this expression is derived by inserting Eqs. (15)–(18) into Eq. (9) and gives a much more concise view of the problem than previous derivations based on individual energy level shifts. Its derivation, also given in the Appendix, is slightly more complex than in the previous case since it involves an uncoupled representation of the spin part in the dipolar interaction, but it still involves the selection rules for the T_{lm} as the main principle. We shall

not give the expression for $V^{(1)}$ since it does not involve cross terms and the main contribution comes from the quadrupolar interaction as in Eq. (14).

With this general tool, the second-order effects clearly show a lattice orientation behavior that is expanded as linear combinations of Wigner matrices of ranks 0, 2, and 4. Trajectories like DAS or DOR can readily be seen to average these anisotropy effects.

By using the appropriate formulas,[19] the present method can be extended to some cases of degenerate systems, provided the number of levels remains small. However, for highly degenerate systems this procedure cannot be used and alternative approaches, for instance, the Van Vleck transformation, must be adopted.[33] We now develop the VVT equations and treat in some detail the case of homogeneous dipolar broadening in a solid.

III. VAN VLECK TRANSFORMATION IN TERMS OF IRREDUCIBLE TENSOR OPERATORS

VVT, which was first applied by Van Vleck to molecular spectroscopy calculations,[33] is a perturbative method used to block diagonalize an operator having groups of degenerate eigenvalues. Block diagonalization means that no off-diagonal elements connect states of different unperturbed eigenvalues. However, no restrictions are set inside each eigenspace, which may be highly degenerate. In an operator formalism this is defined by

$$H=H^{(0)}+H^{(1)}=WDW^{\dagger}, \tag{20}$$

$$[H^{(0)},\ D]=0, \tag{21}$$

$$WW^{\dagger}=\mathbf{1}, \tag{22}$$

where here we denote the tilting matrix by W to indicate that it does not completely diagonalize the Hamiltonian. As in SPT, the perturbation expansion can be written in operator form. The expansion of D is identical to Eq. (9), and it is convenient to expand W as

$$W=\exp(iS^{(1)})\exp(iS^{(2)})\exp(iS^{(3)})\cdots, \tag{23}$$

where the $S^{(n)}$ are Hermitian operators whose magnitudes decrease as $(|H^{(1)}|/|H^{(0)}|)^n$. Such an expansion is at variance with previous treatments,[33,13] but simplifies later calculations. Keeping terms up to the second order, Eq. (20) is expanded as

$$\begin{aligned}H^{(0)}+D^{(1)}+D^{(2)}+\cdots&=\{\mathbf{1}-iS^{(2)}+\cdots)[\mathbf{1}-iS^{(1)}+(iS^{(1)})^2/2+\cdots]\\&\times(H^{(0)}+H^{(1)})(\mathbf{1}+iS^{(1)}+(iS^{(1)})^2/2+\cdots\}\\&\times(\mathbf{1}+iS^{(2)}+\cdots),\end{aligned} \tag{24}$$

and by collecting the various orders yields

$$D^{(1)}=H^{(1)}+[H^{(0)},\ iS^{(1)}], \tag{25}$$

$$D^{(2)}=[H^{(1)},\ iS^{(1)}]+\tfrac{1}{2}[[H^{(0)},\ iS^{(1)}],\ iS^{(1)}]+[H^{(0)},\ iS^{(2)}]. \tag{26}$$

These operator equations do not define the $D^{(n)}$ and $S^{(n)}$ in a unique way [no more than Eqs. (20)–(22) define D and W]. Aside from the trivial case of adding $H^{(0)}$ to $S^{(1)}$ (equivalent to a phase factor on the eigenstates), any other operator commuting with $H^{(0)}$ may be added to a given $S^{(1)}$ to generate another solution. There is no easy way to solve Eqs. (25) and (26) in general. As in SPT, a solution for the $D^{(n)}$ and $S^{(n)}$ was initially given in terms of matrix elements which would eventually yield the expansions for D and W in terms of irreducible tensors.[33] However, in some cases it is possible to directly generate an irreducible tensor solution to Eqs. (20)–(22).

For the case of homogenous dipolar couplings, the Hamiltonians read as

$$H^{(0)}=H_Z=-\omega_Z\sum_i I_Z^{(i)}=-\omega_Z I_Z, \tag{27}$$

$$H^{(1)}=H_D=\sum_{i<j}H_D^{(ij)}=\sum_{i<j}\omega_D^{(ij)}\sum_m(-1)^m R_{2-m}^{(ij)}T_{2\,m}^{(ij)}=\sum_m H_m, \tag{28}$$

where i and j label the spin sites, and the $R^{(ij)}$ and $T^{(ij)}$ are the usual lattice and spin parts of the two-spin coupling. The decomposition of H_D into H_m, introduced by Jeener,[34] is equivalent to the usual dipolar alphabet formalism,[1] and can also be used to represent the quadrupolar interaction treated in Sec. II. An important property of the H_m is their behavior under rotations around Z:

$$[I_Z,\ H_m]=mH_m. \tag{29}$$

As a consequence, another important easily proven relationship follows:

$$\left(I_Z,\prod_n H_{m_n}\right)=\left(\sum_n m_n\right)\left(\prod_n H_{m_n}\right). \tag{30}$$

The relationships in Eqs. (29) and (30) are the key elements to solving Eqs. (25) and (26) in terms of irreducible tensors.

If we set $H^{(1)}=H_D=\Sigma_m H_m$ in Eq. (25), we see that the expression for $D^{(1)}$ has nonsecular contributions ($m\neq 0$) coming from $H^{(1)}$. Since $D^{(1)}$ commutes with $H^{(0)}$, as all $D^{(n)}$, the commutator, $[H^{(0)},\ iS^{(1)}]$, must cancel the nonsecular terms. Using this constraint, Eq. (27) and Eq. (29) can be combined to obtain a simple solution for $S^{(1)}$:

$$S^{(1)}=-\frac{i}{\omega_Z}\sum_{m\neq 0}\frac{H_m}{m}, \tag{31}$$

and thus,

$$D^{(1)}=H_0, \tag{32}$$

where $D^{(1)}$ is the well-known secular part. The solution for higher orders follows the same general procedure: the lower-order terms are inserted, the secular parts are assigned to $D^{(n)}$, and $S^{(n)}$ is tailored to cancel the nonsecular parts by using Eq. (30) in the commutator $[H^{(0)},\ iS^{(n)}]$.

For instance, to get the second-order expressions from Eq. (26), we first introduce $S^{(1)}$, given by Eq. (31), into the first two terms:

$$[H^{(1)},\ iS^{(1)}]+\tfrac{1}{2}[[H^{(0)},\ iS^{(1)}],\ iS^{(1)}]$$
$$=\frac{1}{2\omega_Z}\left(\sum_{m\neq 0}\frac{[H_0,\ H_m]}{m}+\sum_{m\neq 0,\ n\neq 0}\frac{[H_n,\ H_m]}{m}\right), \tag{33}$$

and we identify the secular terms as those with $m+n=0$. Thus

$$D^{(2)}=\frac{1}{\omega_Z}\sum_{m>0}\frac{[H_{-m},\ H_m]}{m}, \tag{34}$$

$$S^{(2)}=\frac{1}{2\omega_Z^2}\left(\sum_{m\neq 0}\frac{[H_0,\ H_m]}{m^2}+\sum_{m\neq n,\ m\neq 0}\frac{[H_{-n},\ H_m]}{m(m-n)}\right). \tag{35}$$

Higher-order corrections, though more complicated, can be computed in a similar way.

Expressions for the VVT expansion to second order have already been found,[34] but the tilting operator $iS^{(1)}$ was not given and the method could not be easily extended to higher orders. A method similar to our VVT operator expansion was previously[35] used to compute $iS^{(1)}$. For homogeneously coupled spin-$\frac{1}{2}$ nuclei the second-order term $D^{(2)}$ [analogous to Eq. (34)] was shown to contain two different parts obtained when expanding the sums over the nuclear indices in the commutators.[34,35] The first part contains two spin contributions, of the $I_Z^{(i)}+I_Z^{(j)}$ type, that only induce a shift of the transition and commute with $D^{(1)}=H_0$. The second part contains three spin contributions that do not shift the line and do not commute with H_0.

The VVT method is not restricted to the dipolar case and can be applied, for instance, to the quadrupolar case treated in the previous section. The prerequisite for VVT to be efficient is the possibility of expanding the perturbation $H^{(1)}$ into contributions which satisfy the commutation relation in Eq. (29). Indeed, the results of the two methods [in Eqs. (13) and (14), and (34), and (31), respectively] are identical for this case and, for higher-order contributions, VVT provides the results in a much simpler way. However, in other cases, VVT may be cumbersome for second-order calculations (for instance, when different spins are involved) or not even tractable if we are interested in a full diagonalization of a degenerate Hamiltonian (in this case SPT could be applied if the number of levels is finite).

IV. GENERATION OF AN EFFECTIVE HAMILTONIAN USING SPT OR VVT

As is well known,[19] the description of a quantum-mechanical system (evolution, observation) is greatly simplified by choosing a reference frame in which the Hamiltonian is in diagonal (or block-diagonal) form. Furthermore, when applying coherent averaging procedures it is often necessary to introduce an interaction representation that, like a propagator, is more easily dealt with in a diagonal basis. Thus, if an exact diagonal form is available for the Hamiltonian, all the calculations can be carried out in the corresponding diagonal reference frame. However, if only approximate diagonalizations are available, it is important to know to what extent this affects the various operations to be carried out. As we shall see, for a given system, different levels of approximation may be necessary depending on the kind of observation and irradiation procedures involved in the experiment.

To analyze the effect of the various approximations, the general procedure is to write the desired equations in the diagonal frame (also referred to as the tilted frame) and then introduce the required perturbation expansions. If the Hamiltonian is diagonalized by a decomposition like Eq. (20), any operator A will be transformed to the tilted frame by the general rule

$$A\rightarrow A^*=W^\dagger A W. \tag{36}$$

Of course, in the particular case of the Hamiltonian, we have $H\rightarrow H^*=D$. In NMR, where the main contribution to the Hamiltonian is the Zeeman interaction, the analysis is simplified by two arguments. First, the application of Eq. (36) is simplified by a perturbation expansion of the operator W in terms of irreducible tensors. Second, the Hamiltonian $H^*=D$ retains the general structure of the I_Z manifolds since it is reduced to the Zeeman interaction in zeroth order. This last statement is obvious but important because it implies that any NMR experiment can be analyzed with the same concepts and tools (rotating frames, averaging techniques, multiple quantum coherences, etc.) that are currently applied to the usual situations (where only first-order expansions without tilting are used). Thus, the system can be described by an effective Hamiltonian, given in the Zeeman eigenbasis by $H^*=D$. However, in this new representation all the operators (density matrix, radio frequency couplings, etc.) are modified by the tilting and may display some unusual properties.

Let us demonstrate this in the simple case of the observation of the free-induction decay. If the initial density matrix is $\rho(0)$ and the observable is I_X, the signal is given by

$$M(t)=\mathrm{Tr}[e^{-iHt}\rho(0)e^{iHt}I_X]$$
$$=\mathrm{Tr}[\rho^*(0)e^{iH^*t}I_X^*e^{-iH^*t}], \tag{37}$$

and the second expression can be reinterpreted as the signal in a Zeeman eigenstate basis with a purely diagonal Hamiltonian H^*, but with modified initial density matrix and observable. The various possible transitions between levels of H^* define the frequency spectrum of $M(t)$, where the amplitudes are proportional to the matrix elements of I_X^*. Thus, the usual $\Delta m=\pm 1$ selection rule, associated with pure I_X, does not apply in general.

However, in standard NMR experiments, the signal is observed with a tuned circuit that selects a band of frequencies around some definite Δm value. Although a general Fourier analysis of $M(t)$ is not easy, the perturbation expansion of the tilting operator W in irreducible tensor form provides a simple decomposition as a function of Δm.

For instance, by expanding W [Eq. (23)] to first order, and then I_X^* [using Eq. (36)], $M(t)$ can be given as

$$M(t)\approx \mathrm{Tr}[\rho^*(0)e^{iH^*t}I_X e^{-iH^*t}] + \mathrm{Tr}[\rho^*(0)e^{iH^*t}[I_X,\ iS^{(1)}]e^{-iH^*t}], \tag{38}$$

where the $S^{(1)}$ terms have been regrouped into a commutator. To zeroth order in W the usual $\Delta m=\pm 1$ rule now applies, and to a small error in the amplitudes we can thus calculate the Zeeman spectrum using the untilted operators and the diagonal effective Hamiltonian, H^*, which in turn can be approximated to any given order. This picture, in which H^* and W are not expanded to the same order, is well suited to NMR experiments, where the frequency resolution can be very high, but the amplitudes of the signals are seldom very accurate.

Equation (38) is also well suited to extract overtones, i.e., contributions other than the $\Delta m=\pm 1$ transitions.[36] These occur to the lowest order from the first-order correction to W, through the term containing $[I_X,\ iS^{(1)}]$ in Eq. (38). For a homonuclear system, $S^{(1)}$ is expanded according to Eq. (23), yielding

$$[I_X,\ iS^{(1)}]=\frac{1}{\omega_Z}\sum_{m\neq 0}\frac{[\frac{1}{2}(I_+ + I_-),\ H_m]}{m} \tag{39}$$

$$=\frac{1}{2\omega_Z}[([I_-,\ H_1]-[I_+,\ H_{-1}]) + \left(\frac{[I_-,\ H_2]-[I_+,\ H_{-2}]}{2}\right) + ([I_+,\ H_1]-[I_-,\ H_{-1}])], \tag{40}$$

where the terms with $\Delta m=0,\ \pm 1$, and ± 2 have been regrouped. Thus we see that the $[I_X,\ iS^{(1)}]$ contribution to the signal will contain zero to two quantum coherences, of which only the $\Delta m=\pm 2$ will be retained in an overtone experiment, and the corresponding signal will then be

$$M_{\text{overtone}}(t)\approx \mathrm{Tr}\left(\rho(0)e^{iH^*t}\frac{1}{2\omega_Z}([I_+,\ H_1] - [I_-,\ H_{-1}])e^{-iH^*t}\right). \tag{41}$$

As in the case of the Zeeman transition we see that the Hamiltonian is diagonal and can be expanded to any order. However, the effective observable is now $(1/2\omega_Z)([I_+,\ H_1]-[I_-,\ H_{-1}])$ instead of I_X.

The addition of a time-dependent perturbation to the Hamiltonian can be handled in a similar manner provided the magnitude of the time-dependent perturbation is small compared to the time-independent part of the Hamiltonian. Let us demonstrate this for the case of rf irradiation. In the tilted representation [Eq. (36)], the Hamiltonian for an rf field of magnitude $2\omega_{\mathrm{rf}}=2\gamma B_{\mathrm{rf}}$ along X can be written as

$$H_{\mathrm{rf}}^*(t)=2\omega_{\mathrm{rf}}\cos(\omega t)I_X^*=\frac{\omega_{\mathrm{rf}}}{2}(e^{i\omega t}+e^{-i\omega t}) \times\left((I_+ + I_-)+\sum_{m\neq 0}\frac{[(I_+ + I_-),\ H_m]}{m\omega_Z}\right), \tag{42}$$

where the second expression was obtained by again expanding the tilting operator, W, to first order using Eqs. (36), (23), and (31). As in the procedure used in the untilted Zeeman case,[1-3] the effect of the pulse is analyzed in a rotating frame, defined by the unitary transformation $e^{-i\omega I_Z t}$:

$$A^*\rightarrow A^\circ = e^{-i\omega I_Z t}A^* e^{i\omega I_Z t}=e^{-i\omega I_Z t}W^\dagger A W e^{i\omega I_Z t}. \tag{43}$$

We shall refer to this representation as the "rotating tilted frame," which should not be confused with the "tilted rotating frame" introduced in the analysis of multiple-pulse experiments.[11,12] The transformed density matrix $\rho^0(t)$ does not contain any high-frequency components, because it evolves under the Hamiltonian

$$H^\circ = H^* + \omega I_Z \tag{44}$$

(since I_Z and H^* commute, H° is reduced to the offset and the local interactions). The effective rf Hamiltonian is obtained from the static parts of Eq. (42) after transformation to the tilted rotating frame using

$$e^{-i\omega I_Z t}I_\pm e^{i\omega I_Z t}=e^{\mp i\omega t}I_\pm,\quad e^{-i\omega I_Z t}H_m e^{i\omega I_Z t}=e^{-im\omega t}H_m, \tag{45}$$

[the second relation is the integrated form of Eq. (29)]. This yields the effective rf Hamiltonian in the rotating tilted frame

$$H_{\mathrm{rf}}^\circ=\omega_{\mathrm{rf}}\left(I_X+\frac{1}{4\omega_Z}(-[I_+,\ H_{-2}]+[I_-,\ H_2])\right) \tag{46}$$

$$=\omega_{\mathrm{rf}}\left(I_X+\frac{1}{2\omega_Z}[I_X,\ H_2+H_{-2}]\right), \tag{47}$$

where the last expression is deduced using the fact that $[I_\pm,\ H_{\pm 2}]=0$.

Similarly, the effect of rf irradiation at the overtone transition frequency can be deduced. Using a $\cos(2\omega t)=\frac{1}{2}(e^{i2\omega t}+e^{-i2\omega t})$ time dependence of the rf field in Eq. (42) and again using Eq. (45), the static part is

$$H_{\mathrm{rf}}^\circ=\frac{\omega_{\mathrm{rf}}}{\omega_Z}([I_+,\ H_1]-[I_-,\ H_{-1}]). \tag{48}$$

As expected the zeroth-order term vanishes leaving the first-order term as the leading contribution. Except for the magnitude ω_{rf}, Eq. (48) is equal to the overtone observable given in Eq. (41). Although the underlying physical phenomena are different, this is not surprising since both the rf and the observable involved the I_X operator in a tilted frame where we applied the same mathematical formalism based on a filtering of the Zeeman frequency multiples.

V. STATIC PERTURBATION THEORIES AND ROTATING SAMPLES

In Sec. IV we introduced the tilted representation and the corresponding effective Hamiltonian H^*. In this representation most experiments can be described, even when higher-order effects are present, within the convenient theoretical environment of fully diagonal interactions (similar to the treatment of first-order perturbations encountered in more common NMR situations). Just as was done to obtain the effective pulse Hamiltonian in Eqs. (47) and (48), a rotating frame can be introduced to eliminate the time dependence due to the Zeeman interaction. In this rotating tilted frame, the system is described by a Hamiltonian H°, as in Eq. (44), which contains only the truncated local interactions. Thus, pulse averaging experiments can be analyzed with the usual tools, e.g., average Hamiltonian theory or secular averaging theory,[11,37,38] applied to H° and the rf-field coupling. At this point, the tilting procedure has no other effects, since the tilting operator W is constant. However, for averaging processes involving sample reorientation (e.g., MAS, DAS, and DOR) the tilting becomes time dependent and deviations from this description can be expected.

In order to study the effects of a time-dependent tilting operator, we begin with the Liouville–von Neumann equation in the laboratory frame and a time-dependent Hamiltonian $H(t)=H^{(0)}+H^{(1)}(t)$, where the local interaction, $H^{(1)}(t)$, is rendered time dependent by the sample motion. Following a derivation adapted from Messiah,[39] we apply a block-diagonalization technique to $H(t)$ for each value of t (for instance, the VVT perturbation expansion presented in the previous section). The corresponding time-dependent tilting operator $W(t)$ defines the usual tilted representation via Eq. (36) for each value of t; in this representation the Liouville–von Neumann equation becomes

$$i\frac{d\rho^*(t)}{dt}=[D(t)+C(t),\rho^*(t)], \tag{49}$$

where

$$C(t)=i\dot{W}^\dagger(t)W(t) \tag{50}$$

and $\dot{W}(t)=dW(t)/dt$. Compared to the static case, the effective Hamiltonian contains the additional term $C(t)$, the magnitude of which depends on both the amount of tilting and the speed of the motion.

Almost all cases of interest for NMR with sample reorientation fall into the adiabatic limit, defined as the vanishingly slow variation of $H(t)$ or, practically, as the vanishingly small ratio of the sample reorientation frequency to the NMR transition frequency. Since the former is typically on the kHz scale while the latter is typically of order MHz, the limit is achieved. In the adiabatic limit we have $|C(t)|\ll|D(t)|$, and a perturbation technique can be applied to the integration of Eq. (49). In first order, D truncates C for every value of t, and only the block diagonal part of it, $B=C_{\text{diag}}$, has to be retained. B is in fact the operator analog of Berry's phase[40,41] if the system is non-degenerate or the non-Abelian generalization of Berry's phase if it is degenerate.[42] The term B arises from the fact that the global geometry of the parameter space describing the spin eigenstates is not flat, and as states evolve in this space they acquire twists (phase shifts) due to the geometry, in addition to the phase shifts due to the dynamic evolution $D(t)$. Put another way, the term B reflects properties of the path followed by the system parameters as they are changed and not the amount of time spent traversing the path (as long as the adiabatic limit is maintained). Deviations from adiabaticity can be handled using perturbation expansions similar to VVT,[39] in this case some mixing of the eigenstates of D occurs, corresponding to excitation of transitions due to $C(t)$. This mixing blurs the respective assignment of dynamic and geometric evolution to $D(t)$ and $C(t)$. In the following, however, we shall only consider the adiabatic limit since it is satisfied in almost all NMR applications involving sample reorientation. Note that the geometric term has been discussed in several previous studies of high-field NMR experiments on rotating solids.[43–45]

The size of the effects introduced by $C(t)$ depends on the amount of tilting, that is, on the extent to which the Zeeman basis defined by the external magnetic field fails to coincide with the eigenvectors of the total Hamiltonian. The limiting case of this failure is pure NQR for which there is no external field. In this case, as has been shown experimentally,[46,47] the spectrum of a rotating sample is qualitatively different from that of a static one: sharp resonances of the static sample split into a finite constant number of sidebands with spacings irrationally related to the spinning frequency. The other limit is zero tilting, realized when higher-order effects are completely negligible. This limit covers, for example, most ^{13}C spectra of organic solids.

For most high-field NMR experiments, the tilting, if nonzero, is small, and the perturbation expansion of W to second order [Eq. (23)] yields

$$C(t)=\dot{S}^{(1)}(t)+\dot{S}^{(2)}(t)+i[\dot{S}^{(1)}(t),\ S^{(1)}(t)]/2+\cdots. \tag{51}$$

Since the leading term of D is the Zeeman interaction, VVT can be applied to the perturbation C. $S^{(1)}$ and $S^{(2)}$, as given in Eqs. (31) and (35), are off diagonal and thus the diagonal part of the commutator term in Eq. (51) is the leading term in the expansion of $B(t)$ and is

$$B^{(1)}(t)=-\frac{i}{2\omega_Z^2}\sum_{m\neq 0}\frac{[\dot{H}_{-m}(t),\ H_m(t)]}{m^2}. \tag{52}$$

For example, in the case of a nucleus of spin greater than $\frac{1}{2}$ with a quadrupole coupling, as considered in Eq. (11), we find

$$B^{(1)}(t)=-\frac{i}{2}\left(\frac{\omega_Q}{\omega_Z}\right)^2 \times\sum_{m\neq 0}\frac{\dot{R}_{2m}(t)R_{2-m}(t)[T_{2-m},\ T_{2m}]}{m^2}. \tag{53}$$

The spin part of this term is equivalent to that of the second-order quadrupolar shift in Eq. (13) and induces shifts of the observed transitions. Since for spinning samples $|\dot{R}_{2\,m}| \sim \omega_R$, with ω_R the spinning frequency, shifts of the resonance lines due to $B^{(1)}$ are of order $\omega_R(\omega_Q/\omega_Z)^2$. Several aspects of this result are worth pointing out. The first is that $B^{(1)}$ represents only the leading term in powers of $|H^{(1)}|$ of the phase shifts due to the geometric evolution. Secondly, we note that the shifts of the resonances due to $B(t)$ are in a sense artifacts of the rotation, in that they are not intrinsic to the local interactions of the spins but rather occur *only* in spinning samples; if these shifts are not removed, erroneous determinations of local interaction parameters, e.g., $e^2qQ/\hbar$, will be made (although as we show later the size of the shifts in practical cases is small). Incidentally, it should also be noted that the small tiltings found in NMR extend the range of the adiabatic behavior. Indeed, for $C(t)$ to be truncated in first order by $D(t)$, only its off-diagonal terms need to be negligible compared to ω_Z. According to the expansion in Eq. (51), this is equivalent to $|\dot{S}^{(1)}| \ll \omega_Z$ or $\omega_R \ll \omega_Z^2/\omega_Q$ in the case of the quadrupolar interaction.

The integration of Eq. (49) is not simple, in general, since typically $D(t)$ and $C(t)$ do not commute with themselves or each other at all times. However, D is in block-diagonal form, with the Zeeman interaction as the leading term and in the adiabatic limit B, the block-diagonal part of C, is retained. As done previously for the case of a static sample, a rotating frame representation given by Eq. (43) can be introduced, where $D^\circ = D + \omega I_Z$, $B^\circ = B$, and the propagator is

$$U^\circ(t) = T \exp\left(-i \int_0^t [D^0(s) + B(s)]\,ds\right). \tag{54}$$

This expression can be simplified in two important cases. If the sample motion is fast enough, dynamic averaging techniques such as AHT, can be applied to obtain an effective static Hamiltonian. In first order one gets

$$\langle D^\circ(s) + B(s)\rangle^{(1)} = \langle D^\circ(s)\rangle^{(1)} + \langle B(s)\rangle^{(1)}, \tag{55}$$

and averages of cross terms enter at higher order. Since typically $|B| \ll |D^\circ|$, most of the Berry's phase effects are described by the first-order term which is decoupled from D°. Another important simple case is found in nondegenerate systems, for which the time ordering of Eq. (54) can be ignored, regardless of the modulation speed. For this case

$$\begin{aligned} U^\circ(t) &= \exp\left(-i \int_0^t [D^\circ(s) + B(s)]\,ds\right) \\ &= \exp\left(-i \int_0^t D^\circ(s)\,ds\right) \exp\left(-i \int_0^t B(s)\,ds\right); \end{aligned} \tag{56}$$

the Berry's phase contribution is again factored out, here rigorously since $[D^\circ, B] = 0$.

A general treatment of a sample undergoing cyclic motion (as in MAS, DAS, and DOR) can be effected by Fourier analyzing the $H_m(t)$ as

TABLE I. Shifts of the central transition as a function of spinning frequency. Parameters are as in Fig. 1. Shown are the line positions of the exact calculation and the second-order SPT calculation (the latter is based on $W = 1$; see text). Shown also are the differences between these calculations and the line shifts induced by the leading geometric correction to the SPT calculation.

Rotor Freq. (Hz)	Exact (Hz)	SPT (Hz)	Exact SPT (Hz)	$\langle B\rangle^{(1)}$ (Hz)
0	390.6	390.6	0	0
2000	196.3	195.3	1.0	1.6
50 000	231.3	195.3	36	39

$$H_m(t) = \sum_p H_{m,p}\, e^{-ip\omega_R t}. \tag{57}$$

Then, the Berry's phase contribution to the average Hamiltonian in first order can be extracted from Eq. (52) as

$$\langle B\rangle^{(1)} = -\frac{\omega_R}{2\omega_Z^2} \sum_{m\neq 0,p} \frac{p[H_{-m,-p},\, H_{m,p}]}{m^2}. \tag{58}$$

Similarly to Eq. (53), in the case of a quadrupolar nucleus of spin greater than $\frac{1}{2}$ this expression yields

$$\langle B\rangle^{(1)} = -\frac{\omega_R}{2}\left(\frac{\omega_Q}{\omega_Z}\right)^2 \times \sum_{m\neq 0,p} \frac{p\; R_{2\,m,p}\; R_{2-m,-p}\; [T_{2-m},\, T_{2\,m}]}{m^2}. \tag{59}$$

We have evaluated this expression numerically for the parameters used in Fig. 1, and show in Table I its effect on the resonance positions. The results of the exact calculation reflect what would be observed experimentally for these parameters, namely, the exact solution of the Liouville–von Neumann equation. Such a solution includes the dynamic effects due to the local parameters of the spin system (the measurement of which is typically the goal of the NMR experiment) and the geometric effects of sample motion (these effects are artifacts, as far as accurate measurement of the nuclear parameters is concerned). The SPT calculation includes second-order effects but neglects all geometric effects. The difference between these calculations arises from higher-order dynamic terms and the geometric term. Comparison of the differences with $\langle B\rangle^{(1)}$ shows that the leading-order geometric correction accounts for much of the discrepancy between the exact and SPT line positions. Moreover, the agreement improves at faster spinning speeds. This trend can be understood by realizing that the third-order term of SPT is of size $\omega_Q(\omega_Q/\omega_Z)^2$ (4.2 Hz for these parameters), which means that at slow spinning speeds ($\omega_R < \omega_Q$) it is the dominant correction, while for fast spinning the Berry's phase term is dominant.

For "typical" experimental parameters of $I = \frac{3}{2}$, $\nu_Z = 50$ MHz, $e^2qQ/\hbar = 3$ MHz, and $\nu_R = 5$ kHz, the leading term of the geometric shift of the central transition is 1.4 Hz, assuming the same orientation of the PAS as was used in the simulations (the third-order SPT term is of the order of 100 Hz). For powder samples, each crystallite will follow a different trajectory, and will thus acquire a different shift.

The geometric term therefore broadens powder patterns, but of course by only a small amount in realistic cases. In practical applications it can be disregarded and the theoretical framework becomes equivalent to that of a static sample, as explored in the previous section, in which the tilting of the eigenstates is neglected.

We close this section by noting that it is likely that the term C represents the fundamental limit of resolution for experiments designed to remove second- and higher-order quadrupolar broadening, such as DAS and DOR. These experiments exploit the symmetries of the eigenvalues of the second-order quadrupolar Hamiltonian; if the geometric term breaks these symmetries, a small residual line broadening will remain. These ideas are currently being investigated quantitatively.

VI. DIFFICULTIES WITH AHT APPROACH TO TRUNCATION

In this last section we will highlight some of the problems associated with the AHT approach to truncation. We begin by describing in what sense AHT provides the "correct answer." The procedure when using AHT for truncation is to first convert the Hamiltonian into the rotating frame,

$$\tilde{H}(t)=e^{iH_Z t}H^{(1)}e^{-iH_Z t}=\sum_m H_m e^{-im\omega_Z t}, \tag{60}$$

where it becomes time dependent and then average it with AHT over the Larmor period, $t_Z=2\pi/\omega_Z$, to obtain the truncated Hamiltonian $\langle H\rangle=\langle H\rangle^{(1)}+\langle H\rangle^{(2)}+\cdots$, to whatever order is necessary. To second order one obtains,[14]

$$\langle H\rangle=H_0+\sum_{m>0}\frac{[H_{-m},\,H_m]}{m\omega_Z}-\sum_{m\neq 0}\frac{[H_0,\,H_m]}{m\omega_Z}+\cdots. \tag{61}$$

The problem with the AHT approach to truncation comes from the assumption that all the observable transitions are actually being observed. This assumption coupled with the stroboscopic nature of AHT results in a folding of multiple quantum transitions into the single quantum spectrum. To emphasize these points an additional set of exact SPT and AHT simulations sampled at multiples of the Larmor period was performed and is shown in Fig. 2. Details of the simulation are given in the Appendix and in the caption of Fig. 2. In all three simulations the spectrum consists of three main Zeeman allowed transitions and three Zeeman forbidden transitions of much less intensity which arise from multiple-quantum transitions that are folded into the spectral window. Both AHT and SPT correctly reproduce all of the frequencies and amplitudes of the exact simulation.

However, while the Zeeman forbidden multiple quantum transitions can be unfolded in the exact and SPT simulations simply by increasing the spectral window, this is not the case in the AHT simulation which must be sampled at multiples of the Larmor period. The multiple quantum lines in the AHT simulation cannot be unfolded with a dwell time shorter than the Larmor period and, in place of AHT, Floquet theory[48] is needed to separate the signal

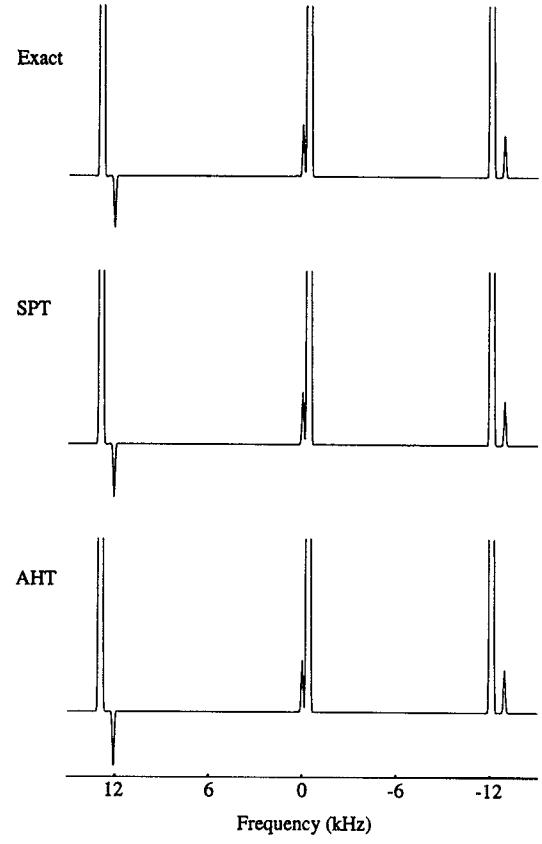

FIG. 2. Exact, SPT, and AHT simulations of the NMR spectrum of a static single-crystal sample, containing equivalent uncoupled quadrupolar nuclei of spin $\frac{3}{2}$. The SPT propagator was calculated as in Fig. 1 but using the tilting operator V expanded to first-order [Eqs. (6), (7), and (14)]. The dwell time in all three simulations is equal to the Larmor period. The vertical scale has been expanded 525 times full scale to show the small Zeeman "forbidden" transitions folded into the $\Delta m=\pm 1$ spectrum. Additional details of the calculation are given in the Appendix.

contributions from the different transition orders. Floquet theory, as described by Maricq,[49] requires the calculation of an additional time-dependent operator, $P(t)$, to yield the effective propagator in the rotating frame,

$$\tilde{U}_F(t)=P(t)e^{-i\langle H\rangle t}, \tag{62}$$

which is valid at all times. When compared to the propagator obtained from SPT or VVT in the rotating frame,

$$\tilde{U}_{\mathrm{VVT}}(t)=e^{iH_Z t}We^{-iDt}W^\dagger=e^{iH_Z t}We^{-iH_Z t}W^\dagger e^{-iWD^\circ W^\dagger t}, \tag{63}$$

one can see the equivalence of these two approaches by setting $P(t)=e^{iH_Z t}We^{-iH_Z t}W^\dagger$ and $\langle H\rangle=WD^\circ W^\dagger$. Note that under conditions of stroboscopic sampling at multiples of t_Z, both propagators reduce to the AHT propagator with the effective Hamiltonian given by Eq. (61), which is equivalent to a second-order expansion of $WD^\circ W^\dagger$,

$$\langle H\rangle=WD^\circ W^\dagger=D^{(1)}+D^{(2)}+i[D^{(1)},\,S^{(1)}]+\cdots. \tag{64}$$

Thus, the truncated Hamiltonian obtained from AHT is correct but, of course, results in spectra that would never be observed in practice since the typical bandwidth of an NMR spectrometer is too small to allow signals over many

megahertz to be aliased into the spectrum. It should be noted, however, that SPT has an advantage over Floquet theory that the perturbation expansion of W in irreducible tensor form allows one to analytically separate the signal contributions from the different transition orders, thus avoiding the short dwell times needed to prevent aliasing of the multiple quantum transitions. When only Zeeman-allowed transitions are needed, W can be simply **1**, and only the calculation of D is required. Floquet theory, however, requires the additional calculation of $P(t)$ even for Zeeman-allowed transitions.

We now focus on the difficulties in treating sample motion when using a truncated Hamiltonian obtained from AHT. If the sample rotation period, t_R, is much larger than the Larmor period, t_Z (a condition equivalent to the adiabatic condition discussed in Sec. V), then the approach taken by others[14,15] is to introduce the time dependence due to sample motion into Eq. (61) to obtain

$$\langle H\rangle(t)=H_0(t)+\sum_{m>0}\frac{[H_{-m}(t),\ H_m(t)]}{m\omega_Z}-\sum_{m\neq 0}\frac{[H_0(t),\ H_m(t)]}{m\omega_Z}+\cdots, \tag{65}$$

and then apply AHT to this expression to obtain an effective time-independent Hamiltonian averaged over the sample motion. This approach is similar to the "second averaging" method[11] where averaging processes of different time scales are treated successively.

The difficulty with this approach is that Eq. (65), just like Eq. (61), has the constraint that it can only be evaluated at integer multiples of the Larmor period. This constraint imposes a discreteness on the motion so that instead of describing a sample undergoing continuous motion, Eq. (65) describes a sample hopping at integer multiples of t_Z between discrete orientations on the trajectory of the continuous motion. When the AHT truncation is only taken to first order, then the approximation of continuous motion by discrete hops at integer multiples of t_Z is a valid one. However, when the AHT truncation is taken beyond first order, the approximation of continuous motion by discrete hops at integer multiples of t_Z requires such restrictive constraints over the normal adiabatic contraints that Eq. (65) has limited utility.

Without making any restrictive assumptions on the motion or the order of the perturbation expansions, we can show the conditions under which Eq. (65) fails to provide a valid approximation for treating sample motion when higher-order truncations are present. As a starting point we introduce the time dependence due to sample motion into Eq. (64), which we showed earlier to be equivalent to Eq. (61), to obtain

$$\langle H\rangle(t)=W(t)D^e(t)W^\dagger(t)=D^{(1)}(t)+D^{(2)}(t)+i[D^{(1)}(t),\ S^{(1)}(t)]+\cdots \tag{66}$$

which is equivalent to Eq. (65). The sample motion, which induces the time dependence of the tilting operator $W(t)$, can be taken into account using a tilted representation, as was done in Sec. V. As in Eq. (49), an effective Hamiltonian in the "tilted rotating frame" can be introduced,

$$\langle H\rangle^*(t)=D^e(t)+C(t), \tag{67}$$

where $C(t)$ is again defined as in Eq. (50). This Hamiltonian describes the system evolution in a "tilted rotating frame" that must not be confused with the rotating tilted frame introduced previously, nor with the usual tilted rotating frame used in multiple-pulse experiments.[11,12] Following the derivations in Sec. V, the propagator in the rotating frame can be given as

$$\tilde{U}_{\rm AHT}(nt_z)=W(nt_z)\,Te^{-i\int_0^{nt_z}[D^e(s)+C(s)]\,ds}W^\dagger(0). \tag{68}$$

In contrast, in the adiabatic limit the rigorous expression, deduced from Eq. (54), for the propagator in the rotating frame and sampled at multiples of the Larmor period is

$$\tilde{U}_{\rm exact}(nt_z)=W(nt_z)\,Te^{-\int_0^{nt_z}[D^e(s)+B(s)]\,ds}W^\dagger(0), \tag{69}$$

where $B(t)$ is the Berry's phase term. In Eq. (69) $B(t)$ is obtained in lowest order from truncation of $C(t)$ by $D(t)$, as shown by the Liouville–von Neumann equation in the laboratory frame [Eq. (49)]. However, in the AHT case [with the Hamiltonian in Eq. (67)], the truncation of $C(t)$ in the propagator of Eq. (68) is determined by $D^e(t)$ which does not contain the Zeeman interaction. Thus, depending on the rotation speed and the structure of the interaction Hamiltonian $D^e(t)$, AHT yields a pseudo-Berry's phase term that can deviate significantly from the $B(t)$ predicted by the rigorous description.

For instance, let us examine the simple case of a quadrupolar nucleus of spin $\frac{3}{2}$ (as used in our simulations). Obviously, $C(t)$ can be nonzero only when perturbative corrections beyond first order are required. Since the eigenstates of $D^e(t)$ and H_Z are identical (i.e., they commute), $C(t)$ will be truncated in the same way by $D^e(t)$ in Eq. (68), as it is by H_Z in Eq. (49). Using the expansion of $C(t)$ in Eq. (51) the AHT description in Eq. (68) matches the rigorous propagator of Eq. (69) if $|S^{(1)}|\ll\omega_Q^2/\omega_Z$, or $\omega_R\ll\omega_Q$. For spinning speeds higher than ω_Q, $C(t)$ may become dominant with respect to $D^e(t)$, resulting in the truncation, at least partially, of $D^e(t)$ by $C(t)$. The resulting change of $D^e(t)$ may yield significant distortions of the spectrum as shown by the AHT simulations of Fig. 1. In the case of a highly degenerate system (e.g., homogeneous dipolar couplings), this "pseudoadiabatic" condition is much more restrictive and the description yielded by AHT is even less efficient.

As mentioned earlier, the physical picture that Eq. (65) describes is not a continuous motion but rather is a discrete hopping at integer multiples of the Larmor period along the path of the continuous trajectory. To illustrate this point, exact and AHT simulations of a sample hopped in discrete steps of $\omega_R t_Z$ radians along the MAS trajectory and sampled at integer multiples of the Larmor period are shown in Figs. 3(a) and 3(b), respectively. Details of the simulation are given in the Appendix and in the caption of Fig. 3. The AHT simulation which employs the Hamil-

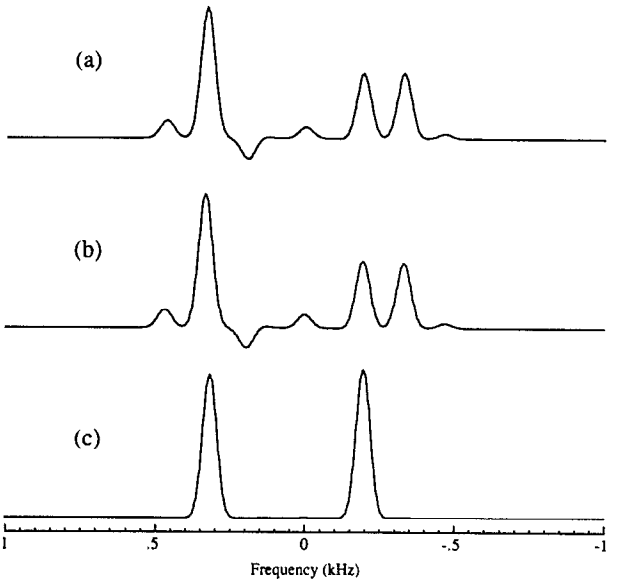

FIG. 3. Exact and AHT simulations of the NMR transitions of a single-crystal sample, containing equivalent uncoupled quadrupolar nuclei of spin $\frac{3}{2}$ hopping along the MAS trajectory in discrete steps of $\omega_R\Delta t$ radians, where $\omega_R=5$ kHz. The dwell time in all three simulations is equal to the Larmor period. Only the region of the central $\pm\frac{1}{2}$ transition is shown. Additional details of the calculation are given in the Appendix. In (a) the exact Hamiltonian was employed to describe a sample hopping along the MAS trajectory at multiples of $\Delta t=t_Z=t_R/100$. In (b) the AHT Hamiltonian given by Eq. (65) was employed to describe a sample hopping along the MAS trajectory at multiples of $\Delta t=t_Z=t_R/100$. In (c) the exact Hamiltonian was employed to describe a sample hopping along the MAS trajectory at multiples of $\Delta t=t_Z/20=t_R/2000$. In the last case the smaller Δt provides a good approximation for a continuous motion about the magic angle.

tonian of Eq. (65) correctly reproduces all of the frequencies and amplitudes in the exact simulation of a sample hopping at integer multiples of the Larmor period. While smaller steps can be employed in an exact simulation to obtain a better approximation of continuous motion, as shown in Fig. 3(c), smaller steps will not provide a better approximation of continuous motion when using the AHT Hamiltonian of Eq. (65). Although the discrete-jump effects obtained in Figs. 3(a) and 3(b) would be difficult to achieve experimentally, they should be carefully considered when performing simulations that involve continuous sample motions. To compute an effective propagator in the case of continuous sample motion, the usual approach consists of approximating the continuous motion as a succession of equal, small discrete jumps, where the Hamiltonian is static for a time Δt. In the limit where Δt goes to zero, this approximation becomes exact. The intuitive constraint might be that Δt be much smaller than the spinning period, t_R. This is indeed a valid constraint if the eigenstates of the Hamiltonian are time independent or if the total propagator can be separated into a dynamic part and a geometric part using the adiabatic approximation described in Sec. V. However, in our exact simulations no adiabatic approximation is made and a single propagator is derived from the complete time-dependent Hamiltonian, and erroneous results could be obtained unless the much more stringent condition $\Delta t \ll t_Z$ is employed.

Although the "second averaging"[11] approach should not be applied using Hamiltonians truncated to higher order with AHT [e.g., Eq. (65)], it can be applied using a Hamiltonian truncated only to first order with AHT since, in this case, the eigenstates will be time independent. When higher-order effects are present an accurate description for a spinning sample can be obtained from AHT provided that the "second averaging" assumption is avoided and the average of the Hamiltonian is calculated in one step over both the Larmor and rotor period. By expanding the time dependence of the complete Hamiltonian in the rotating frame as a Fourier series

$$H(t)=\sum_{p,m} H_{m,p}\ e^{-ip\omega_R t}e^{-im\omega_Z t}, \tag{70}$$

AHT can be applied to this expression to obtain an effective time-independent Hamiltonian averaged over the rotor period, where the rotor period is an integer multiple of the Larmor period. To second order AHT yields an effective Hamiltonian that correctly approximates the dynamic as well as the geometric evolution of the system when sampled stroboscopically at integer multiples of the rotor period.

VII. SUMMARY

We have attempted to present a general and consistent framework for treating higher-order truncations in NMR using SPT and VVT, and have illustrated this with a few examples. By exploiting the fact that the Zeeman interaction, a linear combination of I_Z operators, is the dominant interaction in NMR, irreducible-tensor expansions for the tilting matrix W and the effective Hamiltonian in the tilted frame D are obtained. Irreducible tensor operators simplify these calculations since their commutation relationships with I_Z are simple and matrix elements can be obtained using simple selection rules. Knowledge of W permits one to work in a diagonal frame where operators are modified and consequently display unusual properties (e.g., overtone excitation and detection). Coherent averaging techniques can also be applied in this diagonal frame in the same manner as they are when no tilting is present. In addition, the perturbative expansion of W allows the NMR signal to be "filtered" according to Δm transitions, thus avoiding aliasing problems when using small spectral widths. Sample motion, which creates a time-dependent diagonal basis, can be treated with these techniques using the adiabatic approximation to obtain the dynamic as well as geometric (Berry's phase) evolution of the system. Finally, the difficulties associated with the AHT approach to truncation have been shown to be related to its stroboscopic nature, which aliases multiple quantum transitions into the single quantum spectrum. In addition, we have demonstrated how "second averaging" with AHT to treat multiple time dependencies can sometimes lead to problems when the higher-order effects are involved.

In conclusion, this formalism provides a coherent framework to carry out both analytical and numerical analysis on a wide variety of solid-state NMR experiments where the truncation by the Zeeman interaction involves higher-order effects, for instance, DAS, DOR, or overtone spectroscopy, as well as in more standard methods like MAS.

ACKNOWLEDGMENTS

We wish to thank Alex Pines for helpful discussions. This work was supported by the Director, Office of Energy Research. Office of Basic Energy Sciences, Material Sciences Division of the U. S. Department of Energy under Contract No. DE-AC03-76SF00098. A.L. acknowledges financial support from the Commissariat à l'Energie Atomique, France, and from the North-Atlantic Treaty Organization (Grant No. 68C89FR). P.J.G. acknowledges support from the NIH.

APPENDIX: CALCULATIONS

1. Computation methods

In Figs. 1–3 we show simulations of the NMR transitions of a single-crystal sample, containing equivalent uncoupled quadrupolar nuclei of spin $\frac{3}{2}$, spinning around the magic angle. The quadrupolar interaction is symmetric and its axis is oriented perpendicular to the spinner axis. The quadrupolar frequency (ν_Q=25 kHz) is low enough to observe significant effects at usual spinning speeds and the Zeeman frequency (ν_Z=500 kHz), although not practical in standard NMR, is chosen to yield significant second-order effects.

In all exact simulations the Hamiltonian contained the Zeeman and the complete untruncated quadrupolar interaction as given by Eqs. (10) and (11), respectively. Details on the SPT and AHT Hamiltonians used in the simulations are given in Figs. 1–3.

In cases of a time-dependent Hamiltonian (i.e., for continuous rotation of the sample), the evolution was approximated as a set of discrete evenly distributed orientations. For each orientation the Hamiltonian was static and the propagator for the corresponding time period of duration Δt was obtained by numerical diagonalization. The Δt used in each simulation is given in Figs. 1–3.

Using an initial density operator of I_X, application of successive propagators yielded an FID at a preselected dwell time. The FID was obtained from a trace of the density matrix in the rotating frame with I_+ and then zero filled, apodized, and Fourier transformed. When the density operator was propagated in the laboratory frame it was transformed into the rotating frame before taking the trace. It must be emphasized that for all cases the same computer code (except the rotating frame transformation performed prior to the trace) was used with only different Hamiltonians as matrix inputs.

2. Second-order quadrupole

To derive Eq. (13) from Eq. (9), we expand $E^{(2)}$ in the Zeeman eigenbasis $|j\rangle$:

$$E_j^{(2)}=\frac{1}{\omega_Z}\sum_{j\neq k}\frac{\langle j|H_Q|k\rangle\langle k|H_Q|j\rangle}{k-j}. \tag{A1}$$

Using the irreducible tensor expansion of H_Q in Eq. (A1), we then get

$$E_j^{(2)}=\frac{\omega_Q^2}{\omega_Z}\sum_{m,m'}(-1)^{m+m'}R_{2-m}R_{2-m'}\times\sum_{j\neq k}\frac{\langle j|T_{2m}|k\rangle\langle k|T_{2m'}|j\rangle}{k-j}. \tag{A2}$$

Now we apply the general selection rule for irreducible tensors,

$$\langle k|T_{2m}|j\rangle=\delta_{k,j+m}\langle j+m|T_{2m}|j\rangle, \tag{A3}$$

which restricts the sum over k in Eq. (A2) to the cases where $k=j+m'$ and $k=j-m$. The sum over m and m' is thus also restricted to $m+m'=0$ (with $m\neq 0$) giving

$$E_j^{(2)}=\frac{\omega_Q^2}{\omega_Z}\sum_{m\neq 0}\frac{R_{2-m}R_{2m}}{m}\langle j|T_{2m}|j-m\rangle\times\langle j-m|T_{2-m}|j\rangle. \tag{A4}$$

Using $|j-m\rangle\langle j-m|=\mathbf{1}-\Sigma_{k\neq j-m}|k\rangle\langle k|$, Eq. (A4) becomes

$$E_j^{(2)}=-\frac{\omega_Q^2}{\omega_Z}\sum_{m\neq 0}\frac{R_{2-m}R_{2m}}{m}\langle j|T_{2m}T_{2-m}|j\rangle. \tag{A5}$$

$T_{2m}T_{2-m}$ is a diagonal operator in the Zeeman eigenbasis (transforming as $m=0$ tensors through rotations around Z) and, therefore, commutes with the diagonal projector $|j\rangle\langle j|$. Using Eq. (9) we obtain

$$D^{(2)}=-\frac{\omega_Q^2}{\omega_Z}\sum_{m\neq 0}\frac{R_{2-m}R_{2m}T_{2m}T_{2-m}}{m}. \tag{A6}$$

Splitting the sum over m in Eq. (A6) into two equal parts and regrouping terms of opposite m into commutators, we finally get Eq. (13).

Similarly, the expression for $V^{(1)}$ can be obtained by substituting Eq. (11) into Eq. (5) and obtaining

$$\begin{aligned}|v_j^{(1)}\rangle&=\frac{\omega_Q}{\omega_Z}\sum_m(-1)^m R_{2-m}\sum_{k\neq j}|k\rangle\frac{\langle k|T_{2m}|j\rangle}{j-k}\\&=-\frac{\omega_Q}{\omega_Z}\sum_{m\neq 0}(-1)^m\frac{R_{2-m}}{m}|m+j\rangle\times\langle m+j|T_{2m}|j\rangle\\&=-\frac{\omega_Q}{\omega_Z}\sum_{m\neq 0}(-1)^m\frac{R_{2-m}T_{2m}}{m}|j\rangle,\end{aligned} \tag{A7}$$

$$V^{(1)}=-\frac{\omega_Q}{\omega_Z}\sum_{m\neq 0}(-1)^m\frac{R_{2-m}T_{2m}}{m}. \tag{A8}$$

3. Heteronuclear second-order dipole/quadrupolar

To derive Eq. (19) using the second-order expansion formulas in Eqs. (5) and (9) we start with $H^{(1)}=H_D^{IS}+H_Q^S$ in Eq. (5) and, as explained in the text, we only need to calculate the contribution of the cross terms:

$$ {}^{DQ}E^{(2)}_{m_I m_S} = \sum_{m'_I m'_S \neq m_I m_S} \frac{\langle m_I m_S | H^{IS}_D | m'_I m'_S \rangle \langle m'_I m'_S | H^{S}_Q | m_I m_S \rangle}{E^{(0)}_{m_I m_S} - E^{(0)}_{m'_I m'_S}} + \sum_{m'_I m'_S \neq m_I m_S} \frac{\langle m_I m_S | H^{S}_Q | m'_I m'_S \rangle \langle m'_I m'_S | H^{IS}_D | m_I m_S \rangle}{E^{(0)}_{m_I m_S} - E^{(0)}_{m'_I m'_S}}. \tag{A9} $$

Using the irreducible tensor expressions of the interactions in Eqs. (17) and (18), Eq. (79) then becomes

$$ \begin{aligned} {}^{DQ}E^{(2)}_{m_I m_S} = \omega_D \omega_Q \sum_{m,m',n} (-1)^{m+m'} R^{D}_{2-m} R^{Q}_{2-m'} \langle 1\ 1\ n\ m-n | 1\ 1\ 2\ m \rangle \\ \times \Bigg(\sum_{m'_I m'_S \neq m_I m_S} \frac{\langle m_I m_S | T^{I}_{1\,n} T^{S}_{1\,m-n} | m'_I m'_S \rangle \langle m'_I m'_S | T^{S}_{2\,m'} | m_I m_S \rangle}{(m'_I - m_I)\omega_I + (m'_S - m_S)\omega_S} \\ + \sum_{m'_I m'_S \neq m_I m_S} \frac{\langle m_I m_S | T^{S}_{2\,m'} | m'_I m'_S \rangle \langle m'_I m'_S | T^{I}_{1\,n} T^{S}_{1\,m-n} | m_I m_S \rangle}{(m'_I - m_I)\omega_I + (m'_S - m_S)\omega_S} \Bigg). \end{aligned} \tag{A10} $$

Selection rules for $\langle m_I m_S | T^{I}_{1\,n} T^{S}_{1\,m-n} | m'_I m'_S \rangle$ and $\langle m'_I m'_S | T^{S}_{2\,m'} | m_I m_S \rangle$ give $m_I = n + m'_I$, $m_S = m - n + m'_S$, and $m'_I = m_I$, $m'_S = m' + m_S$, respectively. The combination of these selection rules gives $n=0$, $m+m'=0$, and $m'_S - m_S = -m$, and the condition $m'_I m'_S \neq m_I m_S$ translates as $m \neq 0$. Similar conditions are obtained for the second part of Eq. (80) yielding $n=0$, $m+m'=0$, and $m'_S - m_S = m$. Thus we obtain

$$ \begin{aligned} {}^{DQ}E^{(2)}_{m_I m_S} = -\frac{\omega_D \omega_Q}{\omega_S} \sum_{m \neq 0} \frac{R^{D}_{2-m} R^{Q}_{2\,m}}{m} \langle 1\ 1\ 0\ m | 1\ 1\ 2\ m \rangle (\langle m_I m_S | T^{I}_{1\,0} T^{S}_{1\,m} | m_I m_S - m \rangle \langle m_I m_S - m | T^{S}_{2-m} | m_I m_S \rangle \\ - \langle m_I m_S | T^{S}_{2-m} | m_I m - m_S \rangle \langle m_I m - m_S | T^{I}_{1\,0} T^{S}_{1\,m} | m_I m_S \rangle). \end{aligned} \tag{A11} $$

Since $\langle m_S | T^{S}_{1\pm 2} | m_S \rangle = 0$ the sum over m is restricted to $m = \pm 1$ and the Clebsch–Gordan coefficient becomes $\langle 1\,1\,0 \pm 1 | 1\,1\,2 \pm 1 \rangle = 1/\sqrt{2}$. Again using $|m_I\ m_S - m\rangle\langle m_I\ m_S - m| = \mathbf{1} - \Sigma_{m'_I m'_S \neq m_I m_S - m} |m'_I m'_S\rangle \langle m'_I m'_S|$ we obtain

$$ \begin{aligned} {}^{DQ}E^{(2)}_{m_I m_S} = -(\omega_D \omega_Q / \sqrt{2}\omega_S) \sum_{m=\pm 1} \frac{R^{D}_{2-m} R^{Q}_{2\,m}}{m} \\ \times \langle m_I m_S | T^{I}_{1\,0} [T^{S}_{1\,m}, T^{S}_{2-m}] | m_I m_S \rangle. \end{aligned} \tag{A12} $$

Using $[T_{1\pm 1}, T_{2\mp 1}] = \mp\sqrt{3} T_{2\,0}$, we obtain

$$ \begin{aligned} {}^{DQ}E^{(2)}_{m_I m_S} = -\sqrt{3/2}\, \frac{\omega_D \omega_Q}{\omega_S} \sum_{m=\pm 1} \frac{R^{D}_{2-m} R^{Q}_{2\,m}}{m} \\ \times \langle m_I m_S | T^{I}_{1\,0} T^{S}_{2\,0} | m_I m_S \rangle. \end{aligned} \tag{A13} $$

Substituting this into Eq. (9) we obtain Eq. (19).

In the usual SPT derivations found in the literature,[22–31] the quadrupolar interaction is included in the unperturbed Hamiltonian $H^{(0)}$. This makes the contribution of Eq. (19) appear as a first-order contribution of the dipolar coupling (together with the usual truncated term) over the sum of the Zeeman and quadrupolar interactions. Our approach is slightly different since only the Zeeman interaction is kept as the zeroth-order term. Although theoretically equivalent, the second procedure involves much simpler calculations because the irreducible tensors then display the adequate selection rules between unperturbed eigenstates.

[1] A. Abragam, *Principles of Nuclear Magnetism* (Oxford University, Oxford, 1961).
[2] C. P. Slichter, *Principles of Magnetic Resonance* (Springer-Verlag, Berlin, 1978).
[3] C. A. Fyfe, *Solid-State NMR for Chemists* (C.F.C. Press, Guelph, 1983).
[4] E. R. Andrew, A. Bradbury, and R. G. Eades, *Nature* **182**, 1659 (1958).
[5] I. J. Lowe, Phys. Rev. Lett. **2**, 285 (1959).
[6] J. S. Waugh, L. M. Huber, and U. Haeberlen, Phys. Rev. Lett. **20**, 180 (1968).
[7] U. Haeberlen and J. S. Waugh, Phys. Rev. **175**, 453 (1968).
[8] A. Samoson, E. Lippmaa, and A. Pines, Mol. Phys. **65**, 1013 (1988).
[9] A. Llor and J. Virlet, Chem. Phys. Lett. **152**, 248 (1988).
[10] B. F. Chmelka, K. T. Mueller, A. Pines, J. Stebbins, Y. Wu, and J. W. Zwanziger, Nature **339**, 42 (1989).
[11] M. Mehring, *Principles of High Resolution NMR in Solids* (Springer-Verlag, Berlin, 1976).
[12] U. Haeberlen, *High Resolution NMR in Solids* (Academic, New York, 1976).
[13] M. M. Maricq, Adv. Magn. Reson. **14**, 151 (1990).
[14] M. M. Maricq and J. S. Waugh, J. Chem. Phys. **70**, 3300 (1979).
[15] A. Samoson, E. Kundla, and E. Lippmaa, J. Mag. Reson. **49**, 350 (1982).
[16] E. Kundla, A. Samoson, and E. Lippmaa, Chem. Phys. Lett. **83**, 229 (1981).
[17] A. Samoson and E. Lippmaa, J. Magn. Reson. **84**, 410 (1989).
[18] S. Ganapathy, S. Schramm, and E. Oldfield, J. Chem. Phys. **77**, 4360 (1982).
[19] C. Cohen-Tannoudji, B. Diu, and F. Laloë, *Quantum Mechanics* (Wiley, New York, 1977).
[20] M. E. Rose, *Elementary Theory of Angular Momentum* (Wiley, New York, 1955).
[21] A. R. Edmonds, *Angular Momemtum in Quantum Mechanics* (Princeton University, Princeton, N.J., 1960).
[22] D. L. VanderHart, H. S. Gutowsky, and T. C. Farrar, J. Am. Chem. Soc. **89**, 5056 (1967).
[23] M. E. Stoll, R. W. Vaughan, R. B. Saillant, and T. Cole, J. Chem. Phys. **61**, 2896 (1974).
[24] S. J. Opella, M. H. Frey, and T. A. Cross, J. Am. Chem. Soc. **101**, 5856 (1979).

[25] J. G. Hexem, M. H. Frey, and S. J. Opella, J. Am. Chem. Soc. **103**, 224 (1981).
[26] A. Naito, S. Ganapathy, and C. A. McDowell, J. Chem. Phys. **74**, 5393 (1981).
[27] N. Zumbulyadis, P. M. Henrichs, and R. H. Young, J. Chem. Phys. **75**, 1603 (1981).
[28] A. Naito, S. Ganapathy, and C. A. McDowell, J. Magn. Reson. **48**, 367 (1982).
[29] J. G. Hexem, M. H. Frey, and S. J. Opella, J. Chem. Phys. 77, 3847 (1982).
[30] A. C. Olivieri, L. Frydman, and L. E. Diaz, J. Magn. Reson. **75**, 50 (1987).
[31] A. C. Olivieri, J. Magn. Reson. **81**, 201 (1989).
[32] S. J. Opella, J. G. Hexem, M. H. Frey, and T. A. Cross, Philos. Trans. R. London Ser. A **299**, 665 (1981).
[33] Van Vleck, Phys. Rev. **33**, 467 (1929).
[34] J. Jeener, H Eisendrath, and R. Van Steenwinkel, Phys. Rev. **133** A, 478 (1964).
[35] M. Goldman, *Spin Temperature and Nuclear Magnetic Resonance in Solids* (Oxford University, London, 1970).
[36] R. Tycko and S. J. Opella, J. Chem. Phys. **86**, 1761 (1987).
[37] L. L. Buishivili and M. G. Menabde, Sov. Phys.—JETP **50**, 1176 (1979).
[38] L. L. Buishivili, G. V. Kobakhidze, and M. G. Menabde, Sov. Phys.—JETP **56**, 347 (1982).
[39] A. Messiah, *Quantum Mechanics* (North-Holland, Amsterdam, 1965), Vol. 2, Chap. 17, p. 744.
[40] A. Shapere and F. Wilczek, *Geometric Phases in Physics* (World Scientific, Singapore, 1989).
[41] J. W. Zwanziger, M. Koenig, and A. Pines, Ann. Rev. Phys. Chem. **41**, 601 (1990).
[42] F. Wilczek and A. Zee, Phys. Rev. Lett. **52**, 2111 (1984).
[43] D. Suter, G. C. Chingas, R. Harris, and A. Pines, Mol. Phys. **61**, 1327 (1987).
[44] Z.-H. Gan and D. M. Grant, Mol. Phys. **67**, 1419 (1989).
[45] M. H. Levitt, D. P. Raleigh, F. Creuzet, and R. G. Griffin, J. Chem. Phys. **92**, 6347 (1990).
[46] R. Tycko, Phys. Rev. Lett. **58**, 2281 (1987).
[47] J. W. Zwanziger, M. Koenig, and A. Pines, Phys. Rev. A **42**, 3107 (1990).
[48] J. H. Shirley, Phys. Rev. **138**, 979 (1965).
[49] M. M. Maricq, Phys. Rev. B **25**, 6622 (1982).